Conformal invariance and critical behavior of the O(n) model on the honeycomb lattice

Murray T. Batchelor*
Instituut Lorentz, Nieuwsteeg 18, Postbus 9506, 2300 RA Leiden, The Netherlands

Henk W. J. Blöte
Laboratorium voor Technische Natuurkunde, Lorentzweg 1, Postbus 5046, 2600 GA Delft, The Netherlands
(Received 31 August 1988)

A seven-vertex model on the honeycomb lattice is solved exactly by the Bethe ansatz method. The vertex model is equivalent to the critical O(n) model on the honeycomb lattice. The equivalence is made exact for lattices wrapped on a cylinder with one finite and one infinite direction, by the introduction of a seam into the vertex model. Thus asymptotic finite-size amplitudes of the critical O(n) model are obtained exactly. Applications of the theory of conformal invariance, which relate these amplitudes to the central charge and critical exponents, confirm the existing results and conjectures for these quantities. The finite-size amplitude corresponding to the temperature exponent was not obtained from the exact solution. However, this amplitude was accurately determined from numerical finite-size results obtained by the transfer-matrix method. This result also agrees with recent predictions.

I. INTRODUCTION

The n-vector or O(n) model in d dimensions describes a system of n-dimensional vector variables with rotationally invariant interactions.[1] A case of special interest is the O(n) model for $d=2$, which is both nontrivial and, at least to some degree, amenable to exact analysis. This model, as well as other models connected to it by rules of universality, exhibits a wide spectrum of interesting physical phenomena. It contains the self-avoiding walk problem along with the Ising, XY, and Heisenberg models as special cases, and is closely related to the cubic, Potts, and Ashkin-Teller models.

While the O(n) model in two dimensions is too complicated to be solved in general, progress can be made if one restricts or "truncates" the interactions in the Hamiltonian, allowing the model to be mapped onto a "loop model."[2] The partition function of this latter model is

$$Z_{\text{loop}}=\sum_{G} t^{N-b} n^{P}, \tag{1.1}$$

where the sum is over all distinct graphs G, with G consisting of a number P of closed and nonintersecting loops. Here N is the total number of sites on the lattice and b is the number of edges covered by a loop. The variable t is a measure of the coupling between the original vector variables. An interesting property of (1.1) is that n may be considered as a continuous variable. Such a generalization of the O(n) model serves to enhance its inherent richness of physical phenomena.

The initial mapping to the loop model, along with a number of plausible assumptions, were used by Nienhuis[3] to demonstrate the asymptotic equivalence of the critical O(n) model on the honeycomb lattice with a Gaussian model and its Coulomb gas representation. This enabled him to derive the critical point and the temperature and magnetic exponents, among others in the interval $-2\le n\le 2$. The temperature exponent is in agreement with an earlier conjecture by Cardy and Hamber.[4] However, a relevant question is whether the critical exponents derived by Nienhuis apply to the O(n) model in general, or to perhaps only a subset, as a consequence of the particular choice of the interactions. A rather powerful method to determine critical exponents numerically is to derive finite-size data by means of a transfer matrix, and to apply finite-size scaling[5,6] or phenomenological renormalization[7] to the data. Results obtained by Kolb *et al.*[8] for the quantum O(n) model agree with the Nienhuis prediction for the O(n) model. Furthermore, a comparison with the n-component cubic model can be made. For $d=2$ and $n<2$, the cubic anisotropy is found to be irrelevant,[9] and subsequently for $n<2$ the n-component cubic model is expected to renormalize to the O(n) fixed point. The finite-size method was applied to this model by Blöte and Nightingale,[10] who constructed a transfer matrix for continuous values of n, and confirmed the validity of the Nienhuis result for the temperature exponent with an accuracy on the order of 10^{-3} for a series of n values between $+2$ and -2. This clearly supports the idea of Nienhuis's results applying to the O(n) and related models in general.

These results provide strong evidence for the precise nature of the critical behavior of the O(n) model. Only an exact solution could remove any remaining doubts. An important step in this direction was recently made by Baxter[11] who evaluated the partition function per site of an equivalent vertex model on the honeycomb lattice. Baxter gives each loop in G [recall Eq. (1.1)] an orientation, which may be visualized by placing arrows on the bonds occupied by G. Thus seven distinct vertices are possible on each of the two sublattices (Fig. 1). The vertex weights are chosen so that summation of the vertex weight products over the two orientations of each loop yields precisely the weight implied by Eq. (1.1). This ver-

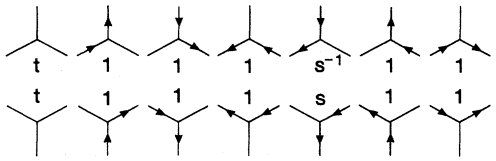

FIG. 1. The allowed arrow and nonarrow configurations for the two types of site, with the corresponding vertex weights. The weight s is defined as $s=e^{6i\alpha}$.

tex model was solved exactly by Baxter using the Bethe ansatz technique under the restriction

$$n=2-(2-t^2)^2 , \tag{1.2}$$

i.e., the criticality condition derived by Nienhuis.[3] Since each loop covers an even number of lattice edges, the sign of t is irrelevant and one may choose $t\geq 0$. On parametrizing t by

$$2\sin 3\alpha = t^2-2 \quad (-\pi/6\leq\alpha\leq\pi/6) , \tag{1.3}$$

it is apparent that α and $-\alpha$ correspond to the same value of n ($n=2\cos 6\alpha$). Thus the solution can be divided into two branches: branch 1 for $\alpha\geq 0$ and branch 2 for $\alpha<0$. According to Nienhuis,[3] branch 1 represents the critical O(n) model, with branch 2 a critical low-temperature phase.

Baxter's interest in the critical O(n) model lay in the thermodynamic limit. It is known[3] that on the honeycomb lattice this model is equivalent to a zero-temperature antiferromagnetic Potts model on the triangular lattice, which in turn is equivalent to the chromatic polynomial of the triangular lattice. This led to the calculation of the large-lattice limit of the chromatic polynomial of the triangular lattice.[11,12] However, the exact mapping of a *finite* O(n) or loop model onto a vertex model may give rise to complications, depending on the boundary conditions. In particular, the bulk weights defined in Fig. 1 do not yield the correct weights for loops closing over the periodic boundaries. Thus the Baxter solution[11] does not contain the finite-size effects of the O(n) model with periodic boundaries (and indeed, nor was it intended to).

Recently much interest exists in such finite-size effects in connection with the theory of conformal invariance and two-dimensional models at criticality.[13] Using the conformal mapping of an infinite plane on an infinitely long cylinder (with a finite cross section) Cardy[14] has related the correlation functions of both systems. Thus he derived a direct relation[15] between the correlation-function exponent η in the infinite plane and the finite-size amplitude of the corresponding correlation length along the cylinder. If these finite-size amplitudes are known for a conformally invariant system, the corresponding scaling dimensions then follow immediately. In addition, a relation has been derived[16,17] between the finite-size amplitude of the singular part of the free energy per site for a system on a cylinder, and the central charge c via the transformation properties of the stress-energy tensor. Furthermore, since the contribution due to the analytic part of the free energy to this amplitude appears to be zero in general,[18] the actual finite-size amplitude of the free energy can be used to determine the central charge of the model. To be specific, if the eigenvalues of the transfer matrix of a system with finite-size L are denoted by $\Lambda_0^{(L)},\Lambda_1^{(L)},\Lambda_2^{(L)},\ldots$ in decreasing order, conformal invariance predicts[16,17] that

$$\ln\Lambda_0^{(L)} = -Lf_\infty + \frac{\pi\xi c}{6L} + \cdots , \tag{1.4}$$

where f_∞ is the reduced bulk free energy per site and ξ is a geometric factor: the ratio between the units of length parallel and perpendicular to the axis of the cylinder [ξ can also account for the effect of anisotropic interactions,[19] and allows for an extension[20] of the results to $(1+1)$-dimensional quantum Hamiltonians]. On the other hand, the ratio of the leading and the ith eigenvalue is found to determine a scaling dimension, X_i, as follows:

$$X_i = \frac{1}{2\pi\xi}\lim_{L\to\infty} L\ln(\Lambda_0^{(L)}/\Lambda_i^{(L)}) . \tag{1.5}$$

If the eigenspectrum of the transfer matrix is known as a function of system size, and the model is indeed conformally invariant, a consistency check is possible because the critical exponents can also be derived from c using the Kac formula[21,22,13] for $c<1$. Parametrizing the central charge by $c=1-6/[m(m+1)]$, the scaling dimensions of the operators in the Virasoro algebra are

$$\Delta_{p,q} = \frac{[p(m+1)-mq]^2-1}{4m(m+1)} , \tag{1.6}$$

where p and q are integers. Exponents associated with rotationally invariant observables (specific heat, susceptibility, ...) satisfy $X_{p,q}=2\Delta_{p,q}$. Thus an exact calculation of the finite-size effects in the O(n) model would be of considerable interest. In this paper, we present such a solution, based on the Bethe ansatz. A brief account of our results has already appeared[23] and the central charge c has also recently been derived by Suzuki,[24] using the same methods.

The passage to the bulk or thermodynamic limit from a discrete set of Bethe ansatz equations to a solvable integral equation was pioneered by Hulthén[25] in his treatment of Bethe's seminal solution of the isotropic linear spin-$\frac{1}{2}$ antiferromagnet.[26] Recently, de Vega and Woynarovich[27] have gone further and given a systematic method for calculating the dominant finite-size corrections to the eigenvalues of any Bethe ansatz soluble model. This method has since been extended and applied to a wide range of critical models. In addition to the *XXZ* Heisenberg chain (or equivalently the six-vertex model),[28–34] the Hubbard chain,[35] and the higher-spin Takhtajan-Babudjian models,[36] the list also includes the eight-vertex,[37,19] Ashkin-Teller,[33] and Potts[32–34] models.

The outline of the paper is as follows. In Sec. II we derive the Bethe ansatz solution of the vertex model, taking particular account of the loops closing over the periodic boundaries. This solution is then used to derive the amplitude of the finite-size correction to the free energy per site, and thus via Eq. (1.4), the central charge c. In

a similar manner we treat a class of excitations which from Eq. (1.5) yield a sequence of scaling dimensions which includes the magnetization and polarization exponents. The section closes with the calculation of the so-called correction-to-scaling exponents, the exponents of which appear as the next leading finite-size correction to the result (1.4). Beyond the analytic results derived in Sec. II, we also give some numerical results for the conformal anomaly and scaling dimensions in Sec. III. These are obtained from the eigenvalues of the transfer matrix by numerically solving the Bethe ansatz equations for finite system size L. In this way we are able to considerably extend the range of finite lattice data obtained by more conventional numerical methods, which are typically restricted to $L \lesssim 15$. However, the solutions of the Bethe ansatz equations that we have obtained do not include the eigenstate associated with the thermal correlation function. Therefore we have used the conventional method to obtain the thermal exponent. These results are also given in Sec. III. In Sec. IV we give a summary and present our conclusions.

II. ANALYTIC RESULTS

We begin this section by considering the vertices of Fig. 1 on the honeycomb lattice depicted in Fig. 2. As motivated above, we are particularly interested in finite periodic lattices (we wrap the lattice on an infinitely long cylinder) for which the loops that close over the periodic boundaries are weighted incorrectly. However, it has been shown in general[38] how this can be overcome by placing a "seam" in the lattice and modifying the weights along the seam. The chosen position of the seam is indicated in Fig. 2 and the corresponding weights, defined along the seam, are shown in Fig. 3. Each oriented loop around the cylinder now acquires an extra weight factor $e^{\pm i\epsilon}$, and summation over the two orientations yields a factor of $2\cos\epsilon$. Thus for $2\cos\epsilon = n$ (i.e., for the particular choice $\epsilon = 6\alpha$), the correct weights are obtained. Fortunately, the introduction of such a seam does not inhibit the Bethe ansatz technique used by Baxter[11] to solve the vertex model.

A. The Bethe ansatz solution

Each of the lattice bonds can be in one of either three states: occupied by an arrow, pointing two possible ways,

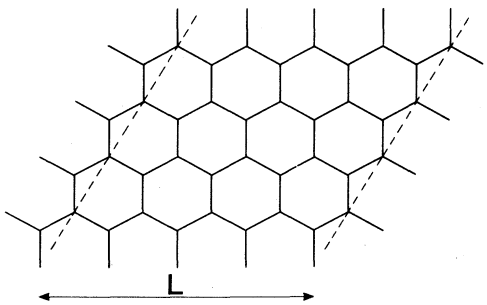

FIG. 2. The periodic honeycomb lattice of width L. Dashed lines indicate the position of the seam.

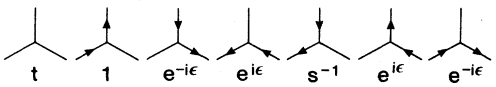

FIG. 3. The modified vertex weights along the seam.

or empty. Now Baxter's approach is to transform the arrows to different types of lines and to subsequently consider the number of lines in each row of vertical edges.[39] For these rows there are either zero, one, or two lines on a bond. Thus a $3^L \times 3^L$ transfer matrix can be defined between two successive rows of vertical edges. In each such row, let there be n_+ (n_-) upward (downward) pointing arrows; then Baxter's number of lines l, defined by $l = L + n_- - n_+$, is the same for each row (conservation of arrows). Consequently the transfer matrix breaks up into $2L+1$ disjoint sectors, each labeled by l.

It is necessary to introduce the seam in the $l = L$ sector, and to do so only in the $l = L$ sector, where loops may indeed close over the periodic boundaries of the cylinder. In other sectors, there is a net arrow flux along the cylinder, and the condition that the loops be nonintersecting prohibits loops winding round the cylinder.

The Bethe ansatz has a long and interesting history.[40] As is customary in applications of the Bethe ansatz, the solution is built up by first considering the sectors $l = 0$, 1, and 2. Following Baxter,[11] we find that the seam only affects his grouping of "right" terms and in general the eigenvalues are given by

$$\Lambda^{(L)} = e^{i\epsilon} \prod_{j=1}^{l} \mu(z_j) + \prod_{j=1}^{l} \nu(z_j) , \tag{2.1}$$

where

$$\mu(z) = 1 - \frac{t^2}{1-z} , \tag{2.2a}$$

$$\nu(z) = \frac{1}{z} + \frac{t^2}{1-z} . \tag{2.2b}$$

Similarly the l parameters z_j are seen to satisfy

$$z_j^L = (-1)^{l-1} e^{i\epsilon} \prod_{k=1}^{l} \frac{S(z_k, z_j)}{S(z_j, z_k)} , \tag{2.3}$$

for $j = 1, \ldots, l$ with

$$S(z,w) = (1 - z - w + zw + t^2 z)(1 - 2w + zw + t^2 w) . \tag{2.4}$$

Thus the eigenspectrum is given by (2.1), with (2.3) the so-called Bethe ansatz equations.

B. The thermodynamic limit

Here our aim is to evaluate the quantity

$$\ln W = \lim_{L \to \infty} \frac{1}{L} \ln \Lambda_0^{(L)} , \tag{2.5}$$

in terms of which the reduced free energy per site is given by $f_\infty = -\ln W$. In order to proceed, a convenient change of variables[11] is

$$z_j = e^{ip_j} = \frac{1+rw_j}{r+w_j} , \tag{2.6}$$

where $r=e^{i\theta}$ with $2\theta=\pi+6\alpha$ and $t^2=2-2\cos\theta$. On further defining $w_j=\exp(2\lambda_j)$, the eigenvalue expression (2.1) can be written

$$\Lambda^{(L)}(\theta,\epsilon)=e^{i\epsilon}\prod_{j=1}^{l}\frac{\sinh(\lambda_j-i\theta)}{\sinh\lambda_j} + \prod_{j=1}^{l}\frac{\sinh(\lambda_j+i\theta)\cosh(\lambda_j-i\theta/2)}{\sinh\lambda_j\cosh(\lambda_j+i\theta/2)} . \tag{2.7}$$

For real λ, (2.6) is equivalent to the substitution

$$p=2\tan^{-1}[\tan(\theta/2)\tanh\lambda] , \tag{2.8}$$

and taking the logarithm in (2.3) gives the equations in the form

$$L\psi(\lambda_j,\theta/2)=2\pi I_j+\epsilon-\sum_{k=1}^{l}\Theta(\lambda_j-\lambda_k) \tag{2.9}$$

for $j=1,\ldots,l$. Here we have defined the function

$$\Theta(\lambda)=\psi(\lambda,\theta/2)+\phi(\lambda,\theta) , \tag{2.10a}$$

where

$$\psi(\lambda,\theta)=2\tan^{-1}(\tan\theta\tanh\lambda) , \tag{2.10b}$$

$$\phi(\lambda,\theta)=2\tan^{-1}(\cot\theta\tanh\lambda) . \tag{2.10c}$$

In (2.9), I_j is an integer for l odd, and half an odd integer for l even. In particular, for the largest eigenvalue in each sector we make the choice

$$I_j=j-(l+1)/2 , \tag{2.11}$$

for $j=1,\ldots,l$ with $l=L$ for the largest overall eigenvalue.

Following deVega and Woynarovich,[27] we introduce the function

$$Z_L(\lambda)=\frac{1}{2\pi}\left[\psi(\lambda,\theta/2)-\frac{\epsilon}{L}+\frac{1}{L}\sum_{k=1}^{l}\Theta(\lambda-\lambda_k)\right] , \tag{2.12}$$

in terms of which the roots λ_j are equally spaced, i.e.,

$$Z_L(\lambda_j)=I_j/L . \tag{2.13}$$

The derivative of (2.12) is denoted by

$$\sigma_L(\lambda)=\frac{dZ_L(\lambda)}{d\lambda} , \tag{2.14}$$

and is directly related to the density of the roots. This asymptotic root density satisfies

$$\sigma_\infty(\lambda)=\frac{1}{2\pi}\psi'(\lambda,\theta/2)+\frac{1}{2\pi}\int_{-\infty}^{\infty}d\mu\,\sigma_\infty(\mu)\Theta'(\lambda-\mu) , \tag{2.15}$$

where the prime denotes differentiation with respect to the λ variable. The integral equation (2.15) can be solved by Fourier transforms. In order to do so, we define in general the Fourier transform pair

$$G(\omega)=\int_{-\infty}^{\infty}g(\lambda)e^{i\omega\lambda}d\lambda , \tag{2.16a}$$

$$g(\lambda)=\frac{1}{2\pi}\int_{-\infty}^{\infty}G(\omega)e^{-i\lambda\omega}d\omega . \tag{2.16b}$$

The solution of (2.15) is

$$\sigma_\infty(\lambda)=\frac{\sqrt{3}a}{\pi}\frac{\sinh(2a\lambda)}{\sinh(3a\lambda)} , \tag{2.17}$$

where we have introduced the quantity

$$a=\frac{2\pi}{3(\pi-\theta)} . \tag{2.18}$$

Given the solution (2.17), and using the definition (2.5), we readily find

$$\ln W=\tfrac{1}{2}\int_{-\infty}^{\infty}d\lambda\,\sigma_\infty(\lambda)f(\lambda) , \tag{2.19}$$

where

$$f(\lambda)=\ln\left[\frac{\cosh2\lambda-\cos2\theta}{\cosh2\lambda-1}\right] . \tag{2.20}$$

Equivalently, (2.19) may be written as[41]

$$\ln W=\frac{1}{4\pi}\int_{-\infty}^{\infty}dx\,\hat{\sigma}_\infty(x)\hat{f}(x) \tag{2.21a}$$

$$=\int_{-\infty}^{\infty}dx\frac{\sinh(\theta x)\sinh(\pi-\theta)x}{x\sinh(\pi x)[2\cosh(\pi-\theta)x-1]} , \tag{2.21b}$$

which is the result obtained by Baxter[11] for $\epsilon=0$, as of course it must be. We have been able to evaluate this integral at two points. These results are $W=2+\sqrt{2}$ at $\theta=3\pi/4$ and $W=2$ at $\theta=\pi/3$, respectively corresponding to self-avoiding walks ($n=0$ on branch 1) and the Ising model in the low-temperature phase ($n=1$ on branch 2).

It is important to realize that the result (2.21b) is only valid in the range $\theta_0<\theta<\pi$ with $\theta_0=0.4279\ldots$.[11,12] Fortunately this covers all of branch 1, and for branch 2 the range $n>-1.311\ldots$. Beyond this point the leading eigenvalue corresponds to a different eigenvector, and subsequently not to the choice of I_j given in (2.11). This crossing of levels results in a "kink" in the bulk free energy as a function of n. We have not yet considered the range beyond this point in any detail.

C. Finite-size corrections

To calculate the dominant finite-size corrections to the eigenvalues, we follow the treatment given by Hamer *et al.*[33] for the modified *XXZ* chain.[42] In parts 1 and 2 of this section, we set out in some detail the calculations for the vertex model with no seam ($\epsilon=0$). The full model with the seam is then a straightforward generalization of these results. This variation is treated in part 3.

1. Largest eigenvalue with no seam ($\epsilon=0$)

Recall that in taking the thermodynamic limit, we were left with the integral equation (2.15), with the solution giving the bulk free energy per site through (2.19). For *finite* L, de Vega and Woynarovich[27] have shown

that the problem can be recast in terms of a similar set of integral equations. We consider the root density (2.14) first. Using the definition (2.12), the *difference* between the finite and the infinite system is, after some manipulation,

$$\sigma_L(\lambda)-\sigma_\infty(\lambda)=\frac{1}{2\pi}\int_{-\infty}^{\infty}d\mu[\sigma_L(\mu)-\sigma_\infty(\mu)]\Theta'(\lambda-\mu)+\frac{1}{2\pi}\int_{-\infty}^{\infty}d\mu\,\Theta'(\lambda-\mu)S_L(\mu)\ , \quad (2.22)$$

where

$$S_L(\mu)=\frac{1}{L}\sum_{j=1}^{l}\delta(\mu-\lambda_j)-\sigma_L(\mu)\ . \quad (2.23)$$

The result (2.22) can be treated as an integral equation in $\sigma_L(\lambda)-\sigma_\infty(\lambda)$, with solution

$$\sigma_L(\lambda)-\sigma_\infty(\lambda)=\int_{-\infty}^{\infty}d\mu\,p(\lambda-\mu)S_L(\mu)\ , \quad (2.24)$$

where

$$p(\lambda)=\int_{-\infty}^{\infty}\frac{d\omega}{2\pi}e^{-i\lambda\omega}\times\frac{\sinh(\theta\omega/2)+\sinh[(\pi-2\theta)\omega/2]}{\sinh(\theta\omega/2)\{2\cosh[(\pi-\theta)\omega/2]-1\}}\ . \quad (2.25)$$

In a similar manner, the difference between the finite-size free energy per site and the limiting expression (2.19) can be written

$$\delta f=\frac{1}{L}\ln\Lambda_0-\ln W=\tfrac{1}{2}\int_{-\infty}^{\infty}J(\mu)S_L(\mu)d\mu\ , \quad (2.26)$$

where

$$J(\mu)=\int_{-\infty}^{\infty}\frac{dx}{x}e^{i\mu x}\frac{2\sinh[(\pi-\theta)x/2]}{2\cosh[(\pi-\theta)x/2]-1}\ . \quad (2.27)$$

This last integral can be evaluated by a standard contour integral in the complex plane, with result

$$J(\mu)=-2\ln\tanh\frac{3a\mu}{2}+3\ln\frac{2\cosh(a\mu)+1}{2\cosh(a\mu)-1}\ , \quad (2.28)$$

where a is defined in (2.18).

Application of the Euler-Maclaurin formula[30,33] to (2.24) and (2.26) leads to

$$\sigma_L(\lambda)-\sigma_\infty(\lambda)=-\left[\int_{-\infty}^{-\Lambda_-}d\mu+\int_{\Lambda_+}^{\infty}d\mu\right]p(\lambda-\mu)\sigma_L(\mu)+\frac{1}{2L}[p(\lambda-\Lambda_+)+p(\lambda+\Lambda_-)]+\frac{1}{12L^2}\left[\frac{p'(\lambda+\Lambda_-)}{\sigma_L(-\Lambda_-)}-\frac{p'(\lambda-\Lambda_+)}{\sigma_L(\Lambda_+)}\right]+O(L^{-4})\ , \quad (2.29)$$

and

$$\delta f=-\tfrac{1}{2}\left[\int_{-\infty}^{-\Lambda_-}d\mu+\int_{\Lambda_+}^{\infty}d\mu\right]J(\mu)\sigma_L(\mu)+\frac{1}{4L}[J(\Lambda_+)+J(-\Lambda_-)]+\frac{1}{24L^2}\left[\frac{J'(\Lambda_+)}{\sigma_L(\Lambda_+)}-\frac{J'(-\Lambda_-)}{\sigma_L(-\Lambda_-)}\right]+O(L^{-4})\ , \quad (2.30)$$

where Λ_+ and $-\Lambda_-$ are the two largest roots in magnitude. For the leading eigenvalue in each sector, corresponding to the choice (2.11), the roots are distributed symmetrically on the real axis, so that $\Lambda_+=\Lambda_-=\Lambda$. In this case (2.29) and (2.30) reduce to

$$\sigma_L(\lambda)-\sigma_\infty(\lambda)=-\int_{\Lambda}^{\infty}d\mu\,p(\lambda-\mu)\sigma_L(\mu)+\frac{p(\lambda-\Lambda)}{2L}-\frac{p'(\lambda-\Lambda)}{12L^2\sigma_L(\Lambda)}+\left[-\int_{-\infty}^{-\Lambda}d\mu\,p(\lambda-\mu)\sigma_L(\mu)+\frac{p(\lambda+\Lambda)}{2L}-\frac{p'(\lambda+\Lambda)}{12L^2\sigma_L(\Lambda)}\right]+O(L^{-4})\ , \quad (2.31)$$

and

$$\delta f=-\int_{\Lambda}^{\infty}d\mu\,J(\mu)\sigma_L(\mu)+\frac{J(\Lambda)}{2L}+\frac{J'(\Lambda)}{12L^2\sigma_L(\Lambda)}+O(L^{-4})\ . \quad (2.32)$$

We now need an expression for Λ. From the definitions (2.12) and (2.14), we find

$$\int_{-\infty}^{\infty}\sigma_L(\lambda)d\lambda=\frac{\theta}{\pi}+\frac{l(\pi-\theta)}{L\pi}\ . \quad (2.33)$$

Thus for the choice (2.11) of the I_j, Λ is determined by

$$Z_L(\Lambda)=\frac{l-1}{2L}\ , \quad (2.34a)$$

or

$$\int_{\Lambda}^{\infty}\sigma_L(\lambda)d\lambda=\frac{1}{2L}\left[1+(L-l)\frac{\theta}{\pi}\right]\ . \quad (2.34b)$$

As for the XXZ chain,[33,34] the bracketed terms in (2.31) are small, and may be neglected in determining the leading-order finite-size corrections as $L\to\infty$. This leaves a Wiener-Hopf equation which is to be solved for the root density $\sigma_L(\lambda)$, subject to the constraint (2.34b). Following Hamer *et al.*,[33] we define

$$k(\lambda)=p(\lambda)\ , \quad (2.35a)$$

$$f(\lambda)=\sigma_\infty(\lambda+\Lambda)\ , \quad (2.35b)$$

$$\chi(\lambda)=\sigma_L(\lambda+\Lambda)\ . \quad (2.35c)$$

Setting $t=\lambda-\Lambda$ in (2.31) then gives the Wiener-Hopf equation,

$$\chi(t)+\int_0^\infty k(t-s)\chi(s)ds=f(t)+\frac{k(t)}{2L}-\frac{k'(t)}{12L^2\sigma_L(\Lambda)} . \tag{2.36}$$

From (2.25) and (2.35a), the kernel of this equation is

$$1+K(\omega)=\frac{\sinh(\pi\omega/2)}{\sinh(\theta\omega/2)\{2\cosh[(\pi-\theta)\omega/2]-1\}} . \tag{2.37}$$

We then use the decomposition

$$\pi/\sin\pi z=\Gamma(z)\Gamma(1-z) , \tag{2.38}$$

to "factorize" (2.37) in the form

$$[1+K(\omega)]^{-1}=G_+(\omega)G_-(\omega) , \tag{2.39}$$

where

$$G_+(\omega)=2\sqrt{\pi\theta}\frac{\Gamma\left[1-i\frac{\omega}{2}\right]e^{h(\omega)}}{\Gamma\left[1-i\frac{\theta\omega}{2\pi}\right]\Gamma\left[\frac{1}{6}-i\frac{(\pi-\theta)\omega}{4\pi}\right]\Gamma\left[\frac{5}{6}-i\frac{(\pi-\theta)\omega}{4\pi}\right]} \tag{2.40a}$$

$$=G_-(-\omega) . \tag{2.40b}$$

Here the functions $G_\pm(\omega)$ are holomorphic and continuous in the upper and lower halves $\pi_\pm$, respectively, of the complex plane. The function $h(\omega)$ is determined by imposing the condition that $G_\pm(\omega)$ are continuous and equal to 1 at $|\omega|\to\infty$ (in $\pi_\pm$, respectively). Using Stirling's formula, we find

$$h(\omega)=\frac{i\omega}{2}\left[\ln\left[\frac{2\pi}{\pi-\theta}\right]-\frac{\theta}{\pi}\ln\left[\frac{2\theta}{\pi-\theta}\right]\right] . \tag{2.41}$$

Then as $|\omega|\to\infty$ in π_+,

$$G_+(\omega)\sim 1+\frac{g_1}{\omega}+\frac{g_2}{\omega^2}+O(\omega^{-3}) , \tag{2.42}$$

where

$$g_1=\frac{i}{3}\left[\frac{1}{2}-\frac{\pi}{2\theta}-\frac{\pi}{3(\pi-\theta)}\right], \quad g_2=\tfrac{1}{2}g_1^2 . \tag{2.43}$$

Finally, at $\omega=0$,

$$G_+(0)=\sqrt{\theta/\pi} . \tag{2.44}$$

Returning now to the Fourier-transformed version of (2.36), we further split the functions $X(\omega)$ and $F(\omega)$ into $\pm$ components (again to be holomorphic and continuous in $\pi_\pm$, respectively), i.e.,

$$X(\omega)=X_+(\omega)+X_-(\omega) , \tag{2.45a}$$

with

$$X_+(\omega)=\int_0^\infty e^{i\omega t}\chi(t)dt , \tag{2.45b}$$

$$X_-(\omega)=\int_{-\infty}^0 e^{i\omega t}\chi(t)dt . \tag{2.45c}$$

The solution of (2.36) is precisely that given in Hamer *et al.*,[33] namely,

$$X_+(\omega)=C(\omega)+G_+(\omega)[P(\omega)+Q_+(\omega)] , \tag{2.46}$$

with

$$C(\omega)=\frac{1}{2L}+\frac{i\omega}{12L^2\sigma_L(\Lambda)} , \tag{2.47}$$

$$P(\omega)=\frac{i(g_1-\omega)}{12L^2\sigma_L(\Lambda)}-\frac{1}{2L} . \tag{2.48}$$

However, due to the different kernel $K(\omega)$, the difference lies in the value of g_1 and also in the function

$$Q_+(\omega)=\frac{G_-(-ia)e^{-a\Lambda}}{\sqrt{3}\left[\frac{\pi}{3}-i(\pi-\theta)\frac{\omega}{2}\right]} . \tag{2.49}$$

The solution (2.46) is now used to determine the finite-size correction. As we are interested in the largest eigenvalue, we take $l=L$ in the constraint (2.34b). Recalling the definitions (2.35c) and (2.45b), this constraint is consistent with the solution (2.46) if $Q_+(0)=-P(0)$, i.e., if

$$\frac{\sqrt{3}}{\pi}G_+(ia)e^{-a\Lambda}=\frac{1}{2L}-\frac{ig_1}{12L^2\sigma_L(\Lambda)} . \tag{2.50}$$

Also from the definition (2.45b) and the solution (2.46), along with the relation $\sigma_L(\Lambda)=\chi(0)=2\chi_+(0)$,[33] we have

$$\sigma_L(\Lambda)=\frac{g_1^2}{24L^2\sigma_L(\Lambda)}+\frac{ig_1}{2L}+\frac{2G_+(ia)e^{-a\Lambda}}{\sqrt{3}(\pi-\theta)} . \tag{2.51}$$

Equation (2.51), together with (2.50), gives a quadratic equation in $\sigma_L(\Lambda)$, with solution

$$\sigma_L(\Lambda)=\frac{1}{L}\left[\frac{\pi}{3(\pi-\theta)}+\frac{ig_1}{2}+\left[\frac{\pi^2}{9(\pi-\theta)^2}+\frac{i\pi g_1}{9(\pi-\theta)}-\frac{g_1^2}{12}\right]^{1/2}\right] , \tag{2.52}$$

showing an explicit $1/L$ dependence. Finally, approximating (2.28),

$$J(\lambda)\sim 6e^{-a\lambda} , \tag{2.53}$$

and using the quadratic in $\sigma_L(\Lambda)$, the equation (2.32) gives rise to

$$\delta f \sim \frac{\sqrt{3}\pi}{12L^2} . \tag{2.54}$$

Thus, with $\xi=\sqrt{3}/2$, the usual[43] geometric factor for the honeycomb lattice, comparison with (1.4) indicates that the central charge is given by $c=1$ for all θ.

2. *Extension to other sectors ($\epsilon=0$)*

The result (2.54) is easily generalized to the other sectors.[33] In doing so, a convenient sector label is $l_s=L-l=0,\pm1,\ldots$; the largest sector having $l_s=0$, etc. Use of the constraint (2.34b) then generalizes (2.50) to

$$\frac{\sqrt{3}}{\pi}G_+(ia)e^{-a\Lambda}=\frac{1}{2L}-\frac{ig_1}{12L^2\sigma_L(\Lambda)}+\frac{l_s\theta}{2L\pi G_+(0)} , \tag{2.55}$$

with $G_+(0)$ given in (2.44). Together with (2.51), and proceeding as for $l_s=0$, this leads to the result

$$\delta f \sim \frac{\sqrt{3}\pi}{12L^2}\left[1-3\left[\frac{l_s\theta}{\pi G_+(0)}\right]^2\right] , \tag{2.56}$$

In this case, comparison with (1.5) gives the set of scaling dimensions

$$X_{l_s}=\frac{l_s^2\theta}{4\pi} . \tag{2.57}$$

3. *Largest eigenvalue with the seam ($\epsilon\neq0$)*

When the phase angle ϵ is nonzero, the root density $\sigma_L(\lambda)$ is no longer symmetric in λ. However, a similar situation occurs in the *XXZ* chain as the result of a "twisted" boundary[33] (see also Ref. 32). In this case $\Lambda_+\neq\Lambda_-$ and the regions $\lambda\geq\Lambda_+$ and $\Lambda\leq-\Lambda_-$ must be considered separately. For the largest eigenvalue ($l_s=0$), the constraints equivalent to (2.34b) are

$$\int_{-\infty}^{-\Lambda_-}\sigma_L(\lambda)d\lambda=\frac{1}{2L}\left[1+\frac{\epsilon}{\pi}\right] , \tag{2.58a}$$

$$\int_{\Lambda_+}^{\infty}\sigma_L(\lambda)d\lambda=\frac{1}{2L}\left[1-\frac{\epsilon}{\pi}\right] . \tag{2.58b}$$

In this case we effectively consider the regions $\lambda\gg\Lambda_+$ and $\lambda\ll-\Lambda_-$. The first difference is that Λ is replaced by $\Lambda_\pm$ in (2.49). Secondly, use of (2.58) replaces (2.50) with

$$\frac{\sqrt{3}}{\pi}G_+(ia)e^{-a\Lambda_\pm}=\frac{1}{2L}-\frac{ig_1}{12L^2\sigma_L(-\Lambda_\pm)}\mp\frac{\epsilon}{2L\pi G_+(0)} . \tag{2.59}$$

Similarly, the analogous result to (2.51) is

$$\sigma_L(\pm\Lambda_\pm)=\frac{g_1^2}{24L^2\sigma_L(\pm\Lambda_\pm)}+\frac{ig_1}{2L}+\frac{2G_+(ia)e^{-a\Lambda_\pm}}{\sqrt{3}(\pi-\theta)} . \tag{2.60}$$

These results are now used in conjunction with the more general expansion (2.30). After some algebra, we arrive at the formula

$$\delta f \sim \frac{\sqrt{3}\pi}{12L^2}\left[1-3\left[\frac{\epsilon}{\pi G_+(0)}\right]^2\right] . \tag{2.61}$$

Comparison with (1.4) now indicates that

$$c=1-3\pi\epsilon^2/\theta , \tag{2.62}$$

which is the desired result. Setting $\epsilon=6\alpha$ and recalling that $2\theta=\pi+6\alpha$, the central charge of the loop model is thus

$$c=1-\frac{3}{\pi\theta}\left[\frac{2\theta}{\pi}-1\right]^2 . \tag{2.63}$$

D. Corrections to scaling

We first consider the result (2.54). The next-leading corrections arise from the approximations made in the derivation. Arguing as for the *XXZ* chain[30,33] these corrections are $O(p(2\Lambda)/L^2)$. For our model, the leading poles of (2.25) are at $\omega=i2\pi/\theta$ and $\omega=ia$, implying

$$p(\lambda)\sim c_1e^{-2\pi\lambda/\theta}+c_2e^{-a\lambda} \text{ as } \lambda\to\infty . \tag{2.64}$$

From the asymptotic root density (2.17),

$$\sigma_\infty(\lambda)\sim\frac{2}{\sqrt{3}(\pi-\theta)}e^{-a\lambda} \text{ as } \lambda\to\infty . \tag{2.65}$$

Using this result in the constraint (2.34b), we find

$$e^{-a\Lambda}\sim\frac{\pi}{2\sqrt{3}L} , \tag{2.66}$$

and so

$$p(2\Lambda)\sim a_1L^{-6(\pi-\theta)/\theta}+a_2L^{-2} \text{ as } L\to\infty . \tag{2.67}$$

Hence finally

$$\delta f=\frac{\sqrt{3}\pi}{12L^2}\left[1+O(L^{-2})+O(L^{-6(\pi-\theta)/\theta})\right] . \tag{2.68}$$

In general, corrections of the same order should appear in the results (2.56) and (2.61). However, in each case the *amplitudes* of these corrections can of course be different. And indeed, as we shall see further below, they may even turn out to be zero.

III. NUMERICAL RESULTS

The numerical solution of *finite* systems of Bethe ansatz equations have also been of recent interest.[44] Such solutions led to, for example, a dramatic increase in the available finite-lattice data in the eight-vertex model[45] and the quantum Hamiltonian versions of the critical Potts and Ashkin-Teller models.[46,47] We now turn to a brief discussion of similar calculations for the O(n) model.

A. Bethe ansatz calculations

In this paper we have considered a particular class of eigenvalues [those corresponding to the choice (2.11)].

For this class, our basic assumption has been that the Bethe ansatz roots λ_j satisfying (2.9) all lie on the real axis in the complex λ plane. This assumption is borne out by our numerical solutions of the Bethe ansatz equations. We first consider the vertex model with no seam ($\epsilon=0$). An initial solution is obtained from the large-t^2 limit in (2.3), or equivalently, neglecting the Θ terms in (2.9). The final solution is then easily obtained by an iteration procedure.[45,46]

To estimate the central charge c, we define the quantity

$$c(L)\equiv\frac{6L^2}{\pi\xi}\left[\frac{1}{L}\ln\Lambda_0^{(L)}+f_\infty\right], \tag{3.1}$$

which, from (1.4), should tend to c as $L\to\infty$. In order to obtain the bulk free energy per site ($-f_\infty=\ln W$), we have evaluated the integral (2.21b) numerically. These results are shown as a function of selected θ in Table I. In Table II, we show the sequence of estimators (3.1) for increasing lattice size and different values of θ. In each case the sequences is clearly approaching the exact value $c=1$ obtained in Sec. II C 1.

There is a technical problem in the evaluation of the largest eigenvalue in the next sector ($l_s=1$). When L is even there are an odd number of zeros (specifically, there are $L-1$), one of which is located at the origin. This zero leads to a divergence when substituted into the eigenvalue expression (2.7). A similar problem occurs in the six- and eight-vertex models and is overcome by taking a derivative and *then* substituting in the zeros.[45] However, here we simply avoid the problem by considering the sector $l_s=1$ for L odd. Conversely, the same problem now exists for the largest overall eigenvalue and as we wish to compute the corresponding scaling dimension, the definition (1.5) cannot be used directly. Instead we now take $c=1$ and combine (1.5) with (1.4). This gives the quantity

$$X_1(L)\equiv\frac{L^2}{2\pi\xi}\left[-f_\infty-\frac{1}{L}\ln\Lambda_0^{(L)}\right]+\frac{1}{12}, \tag{3.2}$$

where by $\Lambda_0^{(L)}$ we mean the largest eigenvalue in the $l_s=1$ sector. The estimators (3.2) are shown in Table III along with the exact value $X_1=\theta/(4\pi)$, obtained in Sec. II C 2 [Eq. (2.57)].

For the $l_s=2$ sector, we return to L even. In Table IV we show the direct finite lattice estimates of the ratio (1.5). In this case (2.57) gives the exact result as $X_2=\theta/\pi$, which is shown for comparison in the table.

TABLE I. Numerical values of the integral (2.21b) appearing in the reduced bulk free energy per site.

θ/π	$\ln W$
$\frac{5}{6}$	1.282 378
$\frac{2}{3}$	$\ln(2+\sqrt{2})=1.227\,947$
$\frac{1}{2}$	0.954 771
$\frac{1}{3}$	$\ln 2=0.693\,147$
$\frac{1}{6}$	0.374 497

TABLE II. Typical finite-size estimates, defined in Eq. (3.1), for the central charge of the seven-vertex model. The exact value is $c=1$, independent of θ.

L \ θ	$5\pi/6$	$\pi/2$	$\pi/6$
2	1.037 650	1.002 272	1.188 357
4	1.009 275	0.997 318	1.100 132
8	1.003 501	0.998 939	1.005 465
16	1.001 544	0.999 712	0.999 042
32	1.000 682	0.999 927	0.999 686
64	1.000 299	0.999 982	0.999 917
128	1.000 131	0.999 995	0.999 979
256	1.000 057	0.999 999	0.999 995

Before turning to nonzero ϵ, we briefly comment on the convergence of the finite lattice estimates. As is apparent in the tables, the convergence is noticeably slower at the point $\theta=5\pi/6$. From Sec. II D, the correction-to-scaling exponent at this point is predicted to be $-\frac{6}{5}$, which is noticeably smaller than the exponent of -2 which dominates the corrections at $\theta=\pi/2$ and $\theta=\pi/6$. In fact the crossover between these two regimes is at $\theta=2\pi/3$ where in analogy to the *XXZ* chain[46,45] we expect corrections $O(L^{-2}\ln L)$. More spectacular however, is the limit $\theta\to\pi$, in which the exponent tends to zero, resulting in the appearance of logarithmic corrections.[30,46,33,34]

The seam variable ϵ effectively "shifts" the levels in the eigenspectrum. For $\epsilon=6\alpha=2\theta-\pi$, as required for the loop model, we show in Table V the estimators (3.1) for typical values of θ on branch 1. The exact value of the central charge is given by the formula (2.63). The point $\theta=3\pi/4$, at which $c=0$, represents something of a peculiarity. Here the finite-size corrections are seen to vanish to *all* orders. A similar point occurs, for example, in the q-state Potts chain at $q=1$.[46,47] These points serve as valuable checks on the numerical solutions, for in this case the Bethe ansatz roots conspire to give $\Lambda_0=(2+\sqrt{2})^L$. Another such point occurs at $\theta=\pi/3$ on branch 2. It is important to emphasize however, that in both cases the rest of the eigenspectrum *does* indeed possess finite-size corrections. With regard to the other points shown in Table V, we see that the convergence of the finite-size estimates is in some cases more rapid than

TABLE III. Typical finite-size estimates, defined in Eq. (3.2), for the scaling dimension associated with the leading eigenvalue in the $l_s=1$ sector of the seven-vertex model. The Exact values are given by $X_1=\theta/(4\pi)$.

L \ θ	$5\pi/6$	$\pi/2$	$\pi/6$
3	0.202 674	0.125 485	0.023 306
5	0.205 057	0.125 101	0.035 651
9	0.206 660	0.125 023	0.041 208
17	0.207 541	0.125 006	0.041 664
33	0.207 973	0.125 001	0.041 671
65	0.208 173	0.125 000	0.041 668
129	0.208 263	0.125 000	0.041 667
257	0.208 302	0.125 000	0.041 667
Exact	0.208 333	0.125 000	0.041 667

TABLE IV. Typical finite-size estimates for the scaling dimension associated with the leading eigenvalue in the $l_s=2$ sector of the seven-vertex model. The exact values are given by $X_2=\theta/\pi$.

L \ θ	$5\pi/6$	$\pi/2$	$\pi/6$
4	0.792 749	0.509 267	0.158 637
8	0.812 151	0.502 356	0.166 262
16	0.823 360	0.500 590	0.166 651
32	0.828 840	0.500 148	0.166 666
64	0.831 348	0.500 037	0.166 667
128	0.832 463	0.500 009	0.166 667
256	0.832 954	0.500 002	0.166 667
Exact	0.833 333	0.5	0.166 667

predicted in Sec. II D. For example, at $\theta=5\pi/6$ and $\theta=2\pi/3$, the convergence appears to be of $O(L^{-4})$. In such cases it appears that the amplitudes of the dominant finite-size corrections simply vanish.

Before proceeding, we need to address the precise correspondence between the loop model and the seven-vertex model with the seam. The mapping implies that the free energies (and hence the conformal charge) of both models map precisely onto each other. However, the subdominant eigenvalues of the transfer matrices may be different. In fact, the eigenvalue spectra cannot match precisely, because the dimensions of the transfer matrices are different. Since ratios of eigenvalues are associated with scaling dimensions, this situation allows the existence of different sets of exponents in the two models. However, the mapping between the O(n), the loop and vertex models also relates the energy-energy and magnetic correlation functions of these models, so that they at least have the associated relevant exponents in common. We will come back to this relation after the definition of the loop-model transfer matrix.

B. O(n) transfer matrix calculations

In order to investigate finite O(n) models in some detail, we have constructed a transfer matrix for the loop model. More precisely, we have devised an algorithm that performs the multiplication of a vector by the transfer matrix. Such an algorithm can be used to find the leading eigenvalues of the transfer matrix, which is nonsymmetric in the case of the loop model. Details can be found, for example, in Ref. 48.

1. Description of the construction

In constructing the loop-model transfer matrix a convenient starting point is Eq. (1.1). Complex weights, which do occur in the seven-vertex model, are thus avoided. Generally, a transfer matrix is defined in terms of the Boltzmann weight of the couplings in and between adjacent rows of the system. Usually, the indices of the transfer matrix are defined directly on the basis of the degrees of freedom in each row. For the loop model, these degrees of freedom take the form of bond variables which assume the value of 1 if the edge is covered by G, and 0 otherwise. The bond variables, however, do not carry enough information to serve as indices of the transfer matrix. The nonlocal interactions implied by Eq. (1.1), due to loops, may depend on bond variables that are far away. Therefore, we use the transfer matrix in the sense of the second definition given by Schultz *et al.*[49] Thus, the index does not represent the state of variables in each row, but rather it contains all of the information necessary to determine the change of energy (or a multiplicative factor to the Boltzmann weight of the system) when a new row is added to the system.

Consider a loop model on a honeycomb lattice wrapped on a cylinder. The axis of the cylinder is chosen parallel to one of the lattice edge directions (the same geometry as in Sec. II). The finite-size L is measured in units equal to the smallest diameter of an elementary hexagon. A row is defined as a ring of L up- and L down-vertices round the cylinder. We consider a cylinder with open ends, with a length of N rows of $2L$ sites, such that there are L dangling bonds at each end of the cylinder. Nonzero bond variables on these dangling bonds must occur pairwise, because the nonzeros form paths that cannot end in the bulk. For simplicity, we assume that at most one nonzero bond variable occurs on one end.

First we consider the case of only zeros. This restriction imposes a boundary condition which is equivalent to the presence of an open end in the spin representation of the O(n) model. This restriction does not apply at the

TABLE V. Finite-size estimates (3.1) with increasing system size for the central charge of the loop and critical O(n) models. The exact values shown are from Eq. (2.63) with $n=-2\cos 2\theta$.

L \ n \ θ/π	$-1.732\ldots$ $\frac{11}{12}$	-1 $\frac{5}{6}$	0 $\frac{3}{4}$	1 $\frac{2}{3}$	$1.732\ldots$ $\frac{7}{12}$
4	−1.247 237	−0.600 549	0	0.500 851	0.855 807
8	−1.261 230	−0.600 032	0	0.500 049	0.856 730
16	−1.267 648	−0.600 002	0	0.500 003	0.857 021
32	−1.270 471	−0.600 000	0	0.500 000	0.857 111
64	−1.271 714	−0.600 000	0	0.500 000	0.857 135
128	−1.272 267	−0.600 000	0	0.500 000	0.857 141
Exact	$-\frac{14}{11}$ $=1.2727\ldots$	$-\frac{3}{5}$	0	$\frac{1}{2}$	$\frac{6}{7}$ $=0.857\,143$

other end of the cylinder. The way in which the nonzeros are distributed, and in which they are pairwise connected (via a path in G_N on the row 1 to N) is called the "connectivity." It is this quantity which carries precisely the information needed to determine the indices of the transfer matrix. Let us now consider the increase in energy of the loop model when a new row of vertices is added to the lattice. According to Eq. (1.1), a reduced energy $\ln n$ is associated with each loop closed by the vertices in the new row, and a reduced energy $\ln t^{-1}$ which each nonzero bond variable. Given the connectivity α_N on the L dangling bonds of the N-row lattice, and the $2L$ vertices in row $N+1$, the energy contribution follows immediately. Besides, it is possible to determine the connectivity α_{N+1} on the new set of dangling bonds due to the graph G_{N+1} on rows 1 to $N+1$. These ingredients suffice to find the transfer matrix $T(\alpha_{N+1},\alpha_N)$ for finite L.

Thus we have constructed an algorithm which maps the c_L allowed connectivities on the integers $1,2,\ldots,c_L$. We have used a sparse matrix representation of $\mathbf{T}$, which leads to a large reduction in computer time and memory requirements. Details will be given elsewhere.[50] In this way, the two dominant eigenvalues of $\mathbf{T}$ were obtained for system sizes up to $L=15$. These eigenvalues determine the free energy and the energy-energy correlation length. The first quantity served to check the numerical Bethe ansatz results for small systems. The second quantity is also of interest since it is not included in the exact results derived in Sec. II. It will be used to determine the temperature dimension X_T [via Eq. (1.5)]. The leading eigenvalues of $\mathbf{T}$ correspond to eigenvalues of the vertex model in the $l_s=0$ sector (i.e., where the number of up arrows equals the number of down-arrows).

Secondly, we consider the case of a single nonzero bond variable on one end of the cylinder. In this case, the other end of the cylinder has, apart from pairwise connected bonds, also a single nonzero bond variable. Thus we had to construct a new algorithm to map the modified connectivities onto the positive integers serving as the indices of a new transfer matrix $\mathbf{T}'$. The graphs G'_N that occur on the N-row cylinder correspond to the graph expansion of the spin-spin correlation function of the O(n) model. Thus the ratio of the largest eigenvalues of $\mathbf{T}$ and $\mathbf{T}'$ determines the magnetic exponent X_H. Using alogrithms similar to those used for $\mathbf{T}$, we were able to determine the leading eigenvalues of $\mathbf{T}'$ for system sizes up to $L=13$. These leading eigenvalues were found to match those of the vertex model transfer matrix in the sectors $l_s=\pm1$, *without* the seam. Thus from Eqs. (1.5), (2.57), and (2.63) the exact result for the magnetic amplitude is

$$X_H=\frac{\theta}{4\pi}-\frac{\pi}{4\theta}\left[1-\frac{2\theta}{\pi}\right]^2, \tag{3.3}$$

with $n=-2\cos 2\theta$ for the O(n) model.

2. *Results for the temperature exponent*

We have calculated the two largest eigenvalues $\Lambda_0^{(L)}$ and $\Lambda_T^{(L)}$ of the loop model transfer matrix, in the manner described above, for system sizes $L=2$ to 13. These calculations were performed for $n=\pm2$, ±1.5, ±1, ±0.5, and 0 on branch 1($\alpha\geq0$) as well as on branch 2($\alpha<0$). In addition, for $n=1$ on branch 2 we also did $L=14$ and $L=15$. The ratio of these two eigenvalues defines a correlation length which can be identified with the energy-energy correlation function. Its finite-size amplitude is simply related to the temperature exponent X_T, and from (1.5), we define a sequence of finite-size estimators as follows:

$$X_T^{(1)}(L)\equiv\frac{1}{2\pi\xi}L\ln(\Lambda_0^{(L)}/\Lambda_T^{(L)}). \tag{3.4}$$

This quantity can be expanded in powers of L^{-1}:

$$X_T^{(1)}(L)=X_T+aL^{-\omega}+\cdots, \tag{3.5}$$

where the ellipsis stands for corrections to scaling with higher powers of L^{-1}. Thus, iterated estimates $X_T^{(2)}(L)$ of X_T are obtained by requiring

$$X_T^{(1)}(L')=X_T^{(2)}(L)+a(L')^{-\omega}, \tag{3.6}$$

for $L'=L$, $L+1$, and $L+2$, so that the three unknowns on the right-hand side can be solved for. The new series of estimates converges more rapidly, but given the maximum value of L, it is shorter. This process can be further iterated until the series becomes too short or until numerical inaccuracies becomes noticeable. Results of this fitting procedure (in most cases $X_T^{(3)}$) are given in Table VI for several values of n on branch 1, and for branch 2 at $n=1.5$ and 1. On branch 2, X_T becomes irrelevant, and the corresponding eigenvalue of the transfer matrix becomes dominated by other eigenvalues as n increases, at least for the system sizes that we could investigate ($L\leq15$). Since our algorithm derives only the two largest eigenvalues for the larger system sizes, we have no results for X_T for $n<1$ on branch 2. For $n=1$, our estimate is based on only one system size: $L=15$. The exact result in Table VI is the original conjecture of Cardy and Hamber,[4,3] which in our notation ($n=-2\cos 2\theta$) reads

$$X_T=2\pi/\theta-2. \tag{3.7}$$

We return to this result in the next section.

TABLE VI. Extrapolated estimates for scaling dimension X_T associated with the thermal exponent of the O(n) model. Estimated uncertainties in the last decimal places are given between parentheses. The expected exact results shown are obtained from Eq. (3.7) with $n=-2\cos 2\theta$.

Branch	n	Estimate	Expected
1	-2	0.03(1)	0
1	-1.5	0.259 7(1)	0.259 955
1	-1	0.400 0(1)	0.4
1	-0.5	0.530 98(2)	0.530 956
1	0	0.666 68(1)	0.666 667
1	0.5	0.817 760(2)	0.817 756
1	1	1.000 000(1)	1.0
1	1.5	1.251 891(1)	1.251 891
1	2	1.999 99(1)	2.0
2	1.5	3.195(1)	3.195 166
2	1	4.1(5)	4.0

IV. CONCLUSION

We have given a Bethe ansatz solution for the eigenvalues of the transfer matrix of a seven-vertex model with a seam. This model is equivalent to a loop model in which the loops closing over the edges of periodic strips are correctly accounted for. The loop model is in turn equivalent to Nienhuis's version of the $O(n)$ model on the honeycomb lattice.[3] We have calculated the leading finite-size corrections in system size to the simplest class of eigenvalues. The vertex model with no seam (i.e., with ordinary periodic boundary conditions) is thus found to be associated with a central charge $c=1$, which is the expected value for models with continuously varying exponents, such as the XXZ chain or six-vertex model. Accordingly, we find that the leading eigenvalue in each sector of the transfer matrix is associated with a scaling dimension varying with θ as given in Eq. (2.57). Given this result, more generally we expect to find the dimensions

$$X_{l_s,m}=\frac{l_s^2\theta}{4\pi}+m^2\frac{\pi}{\theta}\ , \tag{4.1}$$

with $m=0,1,\ldots$ labeling the excitations *within* each sector. Such a structure would then complete the analogy with the result found for the periodic XXZ chain,[46,31] It would indicate that the corresponding operators are again analogs of the Gaussian model operators[51] composed of a "spin-wave" excitation of index l_s and a "vortex" excitation of vorticity m.

The introduction of the seam in the vertex model allows us to identify levels in the eigenspectrum of the loop model. Thus we have derived the central charge of the $O(n)$ model, which is given by Eq. (2.63). In terms of the renormalization coupling constant[3,52] $g=2\theta/\pi$, this result is

$$c(g)=1-6(1-g)^2/g\ , \tag{4.2}$$

which is the value predicted for the $O(n)$ model on the basis of conformal invariance.[53,16] This situation is analogous to the Potts model, for which the presence of the seam in its six-vertex or XXZ equivalent also accounts directly for the variation in c along the critical line.[46,32,33] The leading eigenvalue in the other sectors of the vertex model have an amplitude in the loop model corresponding to

$$X_{l_s}=l_s^2g/8-(1-g)^2/2g\ . \tag{4.3}$$

This result is in agreement with the sequence of exponents found from the mapping to the Coulomb gas.[3,54,52] The magnetization, polarization, and cubic-symmetry-breaking exponents[3] all follow from this sequence. They are given by $X_H=X_{\pm1}$, $X_P=X_{\pm2}$, and $X_{\rm CB}=X_{\pm4}$, respectively.

We have not at present been able to locate the set of Bethe ansatz roots corresponding to the eigenvalue associated with the thermal exponent. Nevertheless, we have verified the result (3.7) to a high degree of accuracy. If the picture is completely analogous to that found in the XXZ chain,[46] as indeed seems likely, then the associated scaling dimensions of the energy and next-leading energy exponents[3] follow from

$$X_T=X_{0,1-3\alpha/\pi}-X_{0,3\alpha/\pi}=4/g-2\ , \tag{4.4}$$

$$X_{TT}=X_{0,2-3\alpha/\pi}-X_{0,3\alpha/\pi}=12/g-4\ , \tag{4.5}$$

where $X_{0,m}$ is as defined in (4.1).

The above results also follow from the Kac formula (1.6) (see, e.g., Ref. 13). The "magnetic" sequence of exponents (4.3) is simply given by[54,52] $X_{l_s}=2\Delta_{l_s,0}$. Similarly the results (4.4) and (4.5) belong to the "thermal" sequence $X_j=2\Delta_{1,2j+1}$. Thus our results are seen to be in precise agreement with the previous work on the Coulomb gas,[3,54,52] and in turn, with the identifications made by assuming conformal invariance.[53]

ACKNOWLEDGMENTS

We would like to thank Dr. B. Nienhuis and Professor J.M.J. van Leeuwen for helpful discussions. We are grateful to Professor P. W. Kasteleyn for discussions on related coloring problems. We are also indebted to Professor R. J. Baxter for pointing out the discontinuity in the bulk free energy in a helpful and patient correspondence. Furthermore, we thank Dr. U. Geigenmüller for helping us with the preparation of the manuscript. This work has been supported by the Stichting voor Fundamenteel Onderzoek der Materie (FOM) which is supported by the "Nederlandse Organisatie voor Zuiver-Wetenschappelijk Onderzoek" (ZWO). M.T.B. has also been supported by the Netherlands Ministry of Education and Science.

*Present address: Department of Theoretical Physics, Research School of Physical Sciences, Australian National University, Canberra, A.C.T. 2601, Australia.

[1]See, e.g., H. E. Stanley, in *Phase Transitions and Critical Phenomena,* edited by C. Domb and M. S. Green (Academic, London, 1974), Vol. 3.

[2]E. Domany, D. Mukamel, B. Nienhuis, and A. Schwimmer, Nucl. Phys. **B190**, 279 (1981).

[3]B. Nienhuis, Phys. Rev. Lett. **49**, 1062 (1982), and in *Phase Transitions and Critical Phenomena,* edited by C. Domb and J. L. Lebowitz (Academic, London, 1987), Vol. 11.

[4]J. L. Cardy and H. W. Hamber, Phys. Rev. Lett. **45**, 499 (1980).

[5]M. E. Fisher, in *Critical Phenomena,* Proceedings of the Enrico Fermi International School of Physics, Vol. 51, edited by M. S. Green (Academic, New York, 1971), pp. 1–99; M. E. Fisher and M. N. Barber, Phys. Rev. Lett. **28**, 1516 (1972).

[6]M. N. Barber, in *Phase Transitions and Critical Phenomena,* edited by C. Domb and J. L. Lebowitz (Academic, London, 1983), Vol. 8.

[7]M. P. Nightingale, J. Appl. Phys. **53**, 7927 (1982).

[8]M. Kolb, R. Jullien, and P. Pfeuty, J. Phys. A **15**, 3799 (1982).

[9]B. Nienhuis, E. K. Riedel, and M. Schick, Phys. Rev. B **27**, 5625 (1983).

[10]H. W. J. Blöte and M. P. Nightingale, Physica A **129**, 1 (1984).

[11]R. J. Baxter, J. Phys. A **19**, 2821 (1986).

[12]R. J. Baxter, J. Phys. A **20**, 5241 (1987).

[13]See the review by J. L. Cardy in *Phase Transitions and Critical Phenomena,* Ref. 3.
[14]J. L. Cardy, J. Phys. A **17**, L385 (1984); Nucl. Phys. **B270**, 186 (1986).
[15]For this relation, see also M. P. Nightingale and H. W. J. Blöte, J. Phys. A **16**, L657 (1983), and references therein.
[16]H. W. J. Blöte, J. L. Cardy, and M. P. Nightingale, Phys. Rev. Lett. **56**, 742 (1986).
[17]I. Affleck, Phys. Rev. Lett. **56**, 746 (1986).
[18]See, e.g., M. R. Dudek, J. M. J. van Leeuwen, and H. W. J. Blöte, Physica A **147**, 344 (1987), and references therein.
[19]D. Kim and P. A. Pearce, J. Phys. A **20**, L451 (1987).
[20]G. von Gehlen, V. Rittenberg, and H. Ruegg, J. Phys. A **19**, 107 (1986).
[21]A. A. Belavin, A. M. Polyakov, and A. B. Zamolodchikov, J. Stat. Phys. **34**, 763 (1984).
[22]D. Friedan, Z. Qiu, and S. Shenker, Phys. Rev. Lett. **52**, 1575 (1984).
[23]M. T. Batchelor and H. W. J. Blöte, Phys. Rev. Lett. **61**, 138 (1988).
[24]J. Suzuki, J. Phys. Soc. Jpn. **57**, 2966 (1988).
[25]L. Hulthén, Arkiv. Mat. Astron. Fys. **26A**, No. 11 (1938).
[26]H. A. Bethe, Z. Phys. **71**, 205 (1931); see also A. Sommerfeld and H. A. Bethe, in *Handbuch der Physik* (Springer, Berlin, 1933), Vol. 24, No. 2, 600–607.
[27]H. J. de Vega and F. Woynarovich, Nucl. Phys. **B251**, 439 (1985).
[28]C. J. Hamer, J. Phys. A **18**, L1133 (1985); **19**, 3335 (1986).
[29]L. V. Avdeev and B. D. Dörfel, J. Phys. A **19**, L13 (1986).
[30]F. Woynarovich and H.-P. Eckle, J. Phys. A **20**, L97 (1987).
[31]F. Woynarovich, Phys. Rev. Lett. **59**, 259 (1987).
[32]H. J. de Vega and M. Karowski, Nucl. Phys. **B285**, 619 (1987); M. Karowski, *ibid.* **B300**, 473 (1988).
[33]C. J. Hamer, G. R. W. Quispel, and M. T. Batchelor, J. Phys. A **20**, 5677 (1987); C. J. Hamer and M. T. Batchelor, *ibid.* **21**, L173 (1988).
[34]C. J. Hamer, M. T. Batchelor, and M. N. Barber, J. Stat. Phys. **52**, 679 (1988).
[35]F. Woynarovich and H.-P. Eckle, J. Phys. A **20**, L443 (1987).
[36]F. C. Alcaraz and M. J. Martins, J. Phys. A **21**, L381 (1988); Phys. Rev. Lett. **61**, 1529 (1988).
[37]C. J. Hamer, J. Stat. Phys. **47**, 331 (1987).
[38]R. J. Baxter, S. B. Kelland, and F. Y. Wu, J. Phys. A **9**, 397 (1976).
[39]We do not reproduce this transformation here, but rather refer the reader to Figs. 3 and 4 of Ref. 11.
[40]For the application to vertex models, see e.g., E. H. Lieb and F. Y. Wu, in *Phase Transitions and Critical Phenomena,* edited by C. Domb and M. S. Green (Academic, London, 1972), Vol. 1, and R. J. Baxter, *Exactly Solved Models in Statistical Mechanics* (Academic, London, 1982).
[41]To avoid confusion, the circumflex denotes a Fourier transform.
[42]As far as possible, we use the same notation for ease of comparison.
[43]See, e.g., V. Privman and M. E. Fisher, Phys. Rev. B **30**, 322 (1984), and Ref. 19.
[44]See, e.g., Refs. 29, 30, 34–36, 45–47, and references therein.
[45]M. T. Batchelor, M. N. Barber, and P. A. Pearce, J. Stat. Phys. **49**, 1117 (1987).
[46]F. C. Alcaraz, M. N. Barber, and M. T. Batchelor, Phys. Rev. Lett. **58**, 771 (1987); Ann. Phys. (N.Y.) **182**, 280 (1988).
[47]F. C. Alcaraz, M. N. Barber, M. T. Batchelor, R. J. Baxter, and G. R. W. Quispel, J. Phys. A **20**, 6397 (1987).
[48]H. W. J. Blöte and M. P. Nightingale, Physica A **112**, 405 (1982).
[49]T. D. Schultz, D. C. Mattis, and E. H. Lieb, Rev. Mod. Phys. **36**, 856 (1964).
[50]H. W. J. Blöte and B. Nienhuis, Physica A (to be published).
[51]L. P. Kadanoff and A. C. Brown, Ann. Phys. (N.Y.) **121**, 318 (1979).
[52]B. Duplantier, J. Stat. Phys. **49**, 411 (1987).
[53]V. S. Dotsenko and V. A. Fateev, Nucl. Phys. **B240**, 312 (1984); V. Singh and B. S. Shastry, Pramana **25**, 519 (1985).
[54]H. Saleur, J. Phys. A **19**, L807 (1986); P. Di Francesco, H. Saleur, and J.-B. Zuber, J. Stat. Phys. **49**, 57 (1987).